

Millennial-centennial Scales Climate Changes of Holocene Indicated by Magnetic Susceptibility of High-resolution Section in Salawusu River Valley, China

LU Yingxia¹, LI Baosheng^{1,2}, WEN Xiaohao¹, QIU Shifan³, WANG Fengnian¹, NIU Dongfeng¹, LI Zhiwen¹
(1. Geography Department, South China Normal University, Guangzhou 510631, China; 2. State Key Laboratory of Loess and Quaternary Geology, Institute of Earth Environment, Chinese Academy of Sciences, Xi'an 710061, China; 3. Guangzhou Institute of Geochemistry, Chinese Academy of Sciences, Guangzhou 510640, China)

Abstract: The upmost segment (Holocene series) of the Milanggouwan stratigraphic section (MGS1) in the Salawusu River valley shows 11 sedimentary cycles of dune sands and fluvio-lacustrine facies, or dune sands and paleosols. The analysis of the magnetic susceptibility of this segment suggests that there are 11 magnetic susceptibility cycles with the value alternating from low to high, in which the layers of the dune sands correspond to the lower value of the magnetic susceptibility and the layers of fluvio-lacustrine facies and paleosols correspond to the higher peaks. The study reveals that the low and high magnetic susceptibility values indicate the climate dominated by cold-arid winter monsoon and warm-humid summer monsoon of East Asia, respectively, and the study area has experienced at least 22 times of millennial-centennial scales climate alternation from the cold-arid to the warm-humid during the Holocene. In terms of the time and the climate nature, the variations basically correspond to those of the North Atlantic and some records of cold-warm changes in China as well. They might be caused by the alternation of winter and summer monsoons in the Mu Us Desert induced by global climate fluctuations in the Holocene.

Keywords: MGS1 segment; magnetic susceptibility; millennial-centennial scales climate changes; Holocene; Salawusu River valley

1 Introduction

Since the 1990s, high-resolution paleoclimate records from Greenland ice core (O'Brien *et al.*, 1995) and terrestrial sediments in Afro-Asian arid area (Guo *et al.*, 1999) and marine sediments in the South China Sea (Wang *et al.*, 1999) have proved one after another that climate changes on millennial-centennial scales occurred from the Late Quaternary-Holocene, and the instability of climate is similar to the Dansgaard/Oeschger oscillation.

The instability of the climate of the Holocene in the mid-latitude regions of China, which was strongly influenced by East Asia monsoon, was also recorded in the ice core (Yao and Shi, 1992), the lacustrine sediment (Chen *et al.*, 2001) and the peat (Xian *et al.*, 2006). The vast areas of deserts in the northern China are ecologi-

cally fragile areas that are strongly influenced by winter monsoon, and the extent and the reversion of desertification in those areas are also restrained by the frequency and the strength of summer monsoon. Therefore, it is significant to study the occurrence of the instable climate of the Holocene in this area to understand the relations between global climate changes of the Holocene and East Asia monsoon environmental evolution in desert areas of China.

The Salawusu River valley (37°20'–37°58'N, 108°08'–108°48'E), situated in the southeastern margin of Mu Us Desert on the Ordos Plateau of Inner Mongolia, China, preserves abundant information on the environmental evolution of East Asia monsoon since the Late Quaternary (Li *et al.*, 1993; 1998), which has been regarded as a standard site for the environmental evolution study since the Late Pleistocene. Early in 1924, French

Received date: 2009-09-09; accepted date: 2010-01-25

Foundation item: Under the auspices of National Basic Research Program of China (No. 2010CB833405), National Natural Science Foundation of China (No. 40772118, 49971009)

Corresponding author: LI Baosheng. E-mail: libsh@scnu.edu.cn

© Science Press and Northeast Institute of Geography and Agroecology, CAS and Springer-Verlag Berlin Heidelberg 2010

paleontologists Teilhard and Licent (1924) characterized the Upper Pleistocene Salawusu (Sjara-Osso-Gol) Formation. In the recent more than 80 years, a great deal of work has been done on the Quaternary stratigraphy, paleontology, paleoanthropology and geochronology, particularly on desert environment evolution in the Salawusu River valley at home and abroad (Jia, 1950; Woo, 1958; Pei and Li, 1964; Qi, 1975; Yuan, 1978; Dong *et al.*, 1982; 1983; Yuan *et al.*, 1983; Li *et al.*, 1987; Liu *et al.*, 2006; Jin *et al.*, 2007; Ouyang *et al.*, 2007). Especially, some researchers in the 1990s came up with that there existed the instable climate of the Holocene in this region based on lacustrine-swampy sediment analysis (Su *et al.*, 1999), which offered some important clues to our deeply study on the millennial-centennial scales climate changes of the Holocene in the Mu Us Desert. This paper, taking the MGS1 segment of the Milanggouwan stratigraphic section as the study object, firstly describes the segment, and then discusses the millennial-centennial scales climate changes of the Holocene based on magnetic susceptibility distribution and its potential causes.

2 Methods

2.1 Study area

The Salawusu River valley is located on the southeastern margin of the Mu Us Desert, which crosses the Ordos Plateau and the Loess Plateau. Based on regionalization of physical geography (Editorial Board of National Atlas of China, 1965), the present bioclimatic zone of the Mu Us Desert (arid desert steppe and semi-arid dry steppe) is a narrow transitional zone between the desert and semi-humid forest steppe. The upper reaches of the Salawusu River flow through hilly land of the Loess Plateau, the middle and lower reaches of it flow through low-lying land which lies in the southeast of the Ordos Plateau. The Salawusu River valley has an average annual precipitation of 350–400 mm. The average monthly temperature is 22°C in July and –9.1°C in January. The direction of surface winds is controlled by the monsoons with cold and dry northwesterly winds in winter and spring, and warm and wet southeasterly winds in summer and autumn.

The Milanggouwan stratigraphic section (37°45'47"N, 108°33'05"E), where the MGS1 segment of this paper lies, is situated in the middle reaches of the Salawusu

River, about 500 m northeast of Milanggouwan Village. The section is from the top of modern mobile sands dune on the Ordos Plateau to the Salawusu River, with a sediment thickness of 83 m, consisting of the Middle Pleistocene Lishi Formation, the Upper Pleistocene Salawusu Formation and Chengchuan Formation, and the Holocene Dagouwan Formation and Dishaogouwan Formation (Li *et al.*, 2004). The MGS1 segments of this section is in the depth of 0–9.44 m.

2.2 Sampling and analysis methods

Based on the detailed description in the field, the MGS1 segment of the Milanggouwan section includes modern dune sands (MD), paleo-mobile dune sands (PD), fluvial facies (FL), lacustrine-swampy facies (LS) and paleosols (PS). There are totally 22 layers in the MGS1 segment from 0MD downward to 21FL, with interbeddings of dune sands and fluvio-lacustrine facies or paleosols (Fig. 1). A total of 162 stratigraphic samples were collected at 5 cm average interval, a few at 4 cm or 7 cm interval for magnetic susceptibility analysis, of which eight stratigraphic samples for ¹⁴C dating and two stratigraphic samples for TL (thermoluminescence) dating.

We measured 162 stratigraphic samples with magnetic susceptibility instrument made in Bartington Company of England at the Laboratory of Geography Department of South China Normal University, Guangzhou, China. The process was as follows: First, the samples were dried and put into a nonmagnetic polystyrene container with a height of 2.5 cm and a diameter of 2.2 cm, then the mass of each sample was weighed. Next, each sample was measured 3 times by magnetic susceptibility instrument, then we could obtain the average value of magnetic susceptibility according to the measuring results for each sample. After that, the average value of magnetic susceptibility was divided by the mass to obtain the final result. Last, all the data were dealt within EXCEL, and the curve of magnetic susceptibility could be plotted.

The eight ¹⁴C Era samples were examined by normal methods with the following materials: mollusk shells from the top of 1PS/LS and 13LS/FL, silts from the middle part of 1PS/LS, the middle and lower parts of 1PS/LS, the bottom of 1PS/LS and from 3LS and 5LS, and organic matters and plant remnants from 11PS. The ¹⁴C age determinations were performed at the ¹⁴C Labo-

ratory of Cold and Arid Regions Environmental and Engineering Research Institute, Chinese Academy of Sciences, Lanzhou, China. These ^{14}C ages have been calibrated by the Int cal 04 database of Calib 5.01 procedure. The two TL ages were dated at the TL Laboratory in Guangzhou Institute of Geochemistry, Chinese Academy of Sciences. The dating material is fine quartz particles of the samples, smaller than $10\ \mu\text{m}$.

3 Chronology of MGS1 Segment and Its Magnetic Susceptibility Distribution

3.1 MGS1 segment and its chronology

From Fig. 1, 11 sedimentary cycles can be seen, each of which consists of a layer of dune sands and its overlying fluvio-lacustrine facies or paleosols (0MD and 21FL as half a cycle) in the MGS1 segment.

The layers at the different depths of the MGS1 segment, their ^{14}C dating results and TL dating results and relative parameters are shown in Table 1, Fig. 1 and Table 2, respectively. The depth of 9.44 m from top to bottom of the

section approaches the interface between the Dagouwan Formation of the Holocene and the Chengchuan Formation of the Upper Pleistocene acknowledged before (Zhou *et al.*, 1982). From Fig. 1, though there is no direct age-dating at the bottom of the Dagouwan Formation (21FL) in MGS1 segment, the age at the top of 18D, $9\ 880\pm 900$ yr TL B.P., approaches the beginning of the Holocene. The left bank of Dishaogouwan ($37^{\circ}43'26''\text{N}$, $108^{\circ}31'02''\text{E}$) which is adjacent to Milangouwan section has the boundary age between Dagouwan Formation and Chengchuan Formation, $9\ 600\pm 160$ yr ^{14}C B.P. (Su and Dong, 1994). Calibrated by Calib 4.4 (Stuiver *et al.*, 1998), it is $10\ 868\pm 392$ cal. yr B.P. However, if the end of the Younger Dryas (i.e., 11 600 yr B.P.) (Taylor *et al.*, 1993) is regarded as the beginning of the Holocene, it might be more appropriate to take 12 000 yr B.P. as the bottom line of the Holocene. In view of the above, the MGS1 segment is the deposition since 12 000 yr B.P., and the age of bottom line of the Holocene of MGS1 segment in this paper is consistent with that from other relative research (Niu *et al.*, 2008).

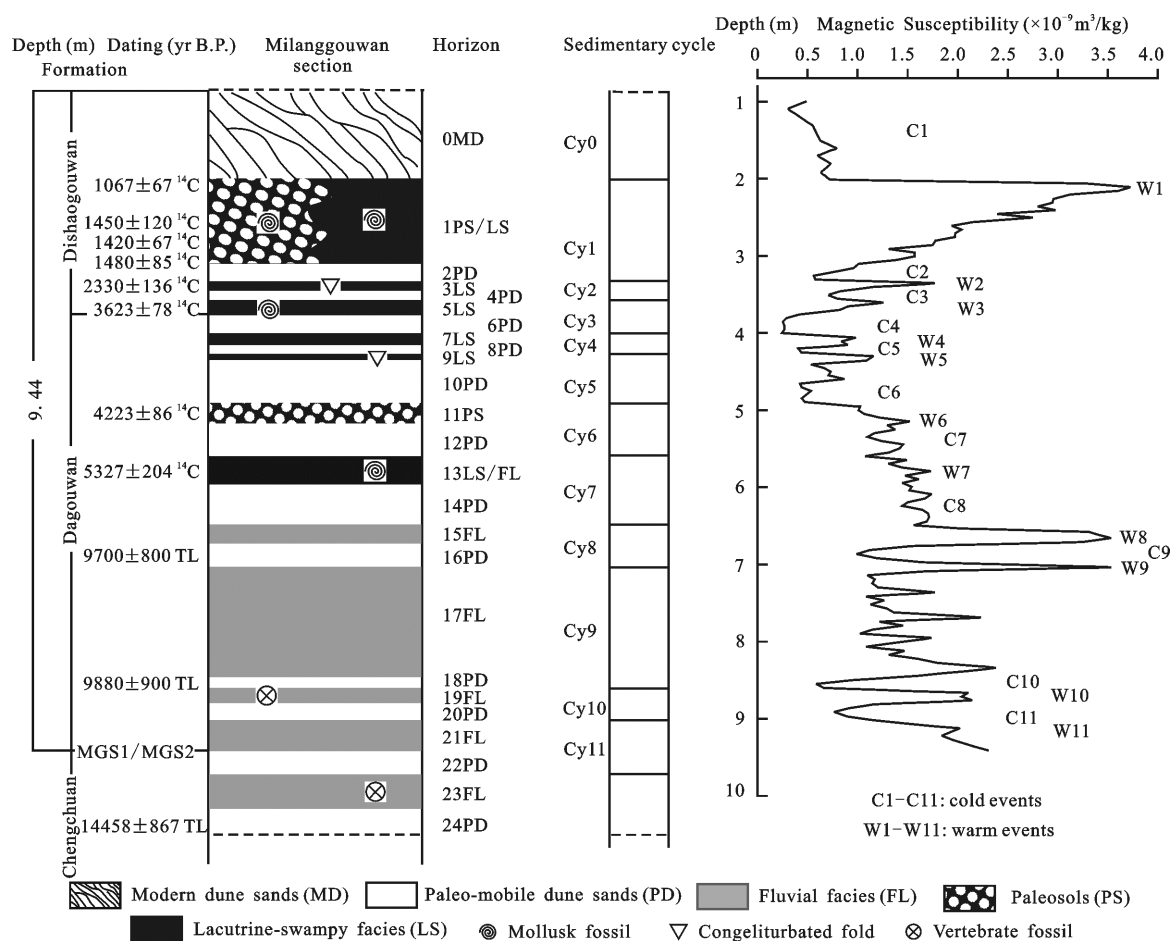


Fig. 1 MGS1 of Milangouwan section and curve of magnetic susceptibility

Table 1 Distribution depth of each horizon and ^{14}C and TL dating of related horizons

Horizon	Depth (m)	Dating results (yr B.P.)	Calendar age (cal. yr B.P.)
0MD	0–2.00		
1PS/LS	2.00–3.05	Top 1067±67*	965 ^{14}C
		Middle 1450±120*	1330 ^{14}C
		Lower middle 1420±67*	1307 ^{14}C
		Bottom 1480±85*	1350 ^{14}C
2PD	3.05–3.30		
3LS	3.30–3.35	Middle 2330±136*	2346 ^{14}C
4PD	3.35–3.55		
5LS	3.55–3.70	Middle 3623±78*	3958 ^{14}C
6PD	3.70–4.00		
7LS	4.00–4.17		
8PD	4.17–4.27		
9LS	4.27–4.32		
10PD	4.32–4.94		
11PS	4.94–5.18	Middle 4223±86*	4828 ^{14}C
12PD	5.18–5.68		
13LS/FL	5.68–5.97	Middle 5327±204*	6170 ^{14}C
14PD	5.97–6.58		
15FL	6.58–6.85		
16PD	6.85–7.08	Bottom 9700±800**	
17FL	7.08–8.49		
18PD	8.49–8.62	Top 9880±900**	
19FL	8.62–8.81		
20PD	8.81–9.04		
21FL	9.04–9.44		

Note: * ^{14}C dating; ** TL dating

3.2 Magnetic susceptibility distribution

As can be seen in Fig. 1 and Table 3, the magnetic susceptibility of the MGS1 segment has three features. First, the magnetic susceptibility values vary extensively from the lowest $24.5 \times 10^{-9} \text{ m}^3/\text{kg}$ to the highest $373.2 \times 10^{-9} \text{ m}^3/\text{kg}$ with an average of $134.3 \times 10^{-9} \text{ m}^3/\text{kg}$ in the whole segment. Secondly, although different in each layer of the same facies, and even in the same horizon, the magnetic susceptibility values of dune sands are relatively low, ranging from $24.5 \times 10^{-9} \text{ m}^3/\text{kg}$ to $174.1 \times 10^{-9} \text{ m}^3/\text{kg}$ with an average of $87.2 \times 10^{-9} \text{ m}^3/\text{kg}$, and those of the fluvio-lacustrine facies and paleosols are relatively high,

ranging from $81.7 \times 10^{-9} \text{ m}^3/\text{kg}$ to $373.2 \times 10^{-9} \text{ m}^3/\text{kg}$ with an average of $183.8 \times 10^{-9} \text{ m}^3/\text{kg}$. Third, the magnetic susceptibility values change from low to high in each sedimentary cycle, lower in the dune sands and higher in the overlying fluvio-lacustrine facies and paleosols. As the dune sands and fluvio-lacustrine facies or paleosols alternating vertically, the curve of the magnetic susceptibility appears fluctuating synchronously with alternative peak-valleys, thus making up 11 magnetic susceptibility cycles which are roughly consistent with the sedimentary cycles.

4 Discussion

The magnetic susceptibility variations mentioned above in different sedimentary facies of the MGS1 segment, particularly the magnetic susceptibility cycles from low to high, which is consistent with the sedimentary cycles rhythm, are similar to those in the sedimentary cycles of loess-paleosol sequence on the Loess Plateau (Liu *et al.*, 1990). In terms of the relationship between magnetic susceptibility and pedogenesis, high magnetic susceptibility represents a strong pedogenesis, whereas low magnetic susceptibility represents a weak pedogenesis, which bears a close relationship to the contents of two primary magnetic minerals, magnetite and hematite. Due to their stability under biochemical weathering, the more warm-humid the climate gets, the more abundant they will be. Such a viewpoint is almost consistent with Kukla's finding that obvious difference of magnetic mineral content occurred in the glacial (loess) and interglacial (paleosol) (Kukla, 1987). In fact, heavy mineral analysis of the Upper Pleistocene and the Holocene series in the Salawusu River valley also greatly supports the magnetic susceptibility variations in different sedimentary facies of the MGS1 segment, i.e., high contents of magnetite and hematite in the fluvio-lacustrine facies and paleosol, and low in dune sands (Li *et al.*, 2000). The average magnetite and hematite contents of dune sands, paleosol and fluvio-lacustrine facies are 5.5%,

Table 2 TL ages and relative parameters of related horizons in MGS1 segment

Horizon (number)	TL age (yr B.P.)	U (ppm)	Th (ppm)	K (%)	E.D. (Gy)	Annual dose (m Gy)
16PD (TGD-781)	9700±800	1.730±0.09	6.130±0.120	1.900±0.015	22±1.650	2.270±0.070
18PD (TGD-627)	9880±900	0.920±0.05	6.070±0.120	1.910±0.015	33.600±2.120	3.400±0.10

Note: Th (thorium) is a natural radionuclides from heavy element; U (uranium), a natural radionuclides from heavy element; K, a natural radionuclides from light element; E.D., equivalent dose

Table 3 Magnetic susceptibility distribution range and average of each horizon

Horizon (sample quantity)	Distribution range ($\times 10^{-9}$ m ³ /kg)	Average ($\times 10^{-9}$ m ³ /kg)
0MD (20)	30.3–79.3	54.5
1PS/LS (21)	129.2–373.2	238.0
2PD (5)	57.5–100.6	77.1
3LS (1)	184.0	184.0
4PD (4)	70.9–116.1	87.2
5LS (3)	81.7–129.3	100.6
6PD (6)	24.5–41.2	28.9
7LS (3)	83.3–98.7	90.9
8PD (2)	40.8–43.6	42.2
9LS (1)	116.8	116.8
10PD (12)	42.1–108.5	61.6
11PS (5)	101.0–153.8	117.4
12PD (9)	105.1–146.0	126.8
13LS/FL (6)	130.4–174.9	151.7
14PD (12)	143.7–174.1	159.7
15FL (5)	204.5–353.9	311.0
16PD (5)	98.1–165.7	130.0
17FL (27)	101.8–358.3	153.3
18PD (3)	58.2–96.7	73.9
19FL (3)	203.7–215.8	210.3
20PD (5)	75.6–116.5	98.0
21FL (4)	184.0–230.7	205.7

Note: 3LS and 9LS layers have one sample respectively

14% and 17.6%, ranging from 1.7% to 9.4%, from 8.3% to 25.5%, and from 10.6% to 29.7%, respectively (Li *et al.*, 2000). Hence, it can be held that the magnetic susceptibility of MGS1 is a good indicator for reflecting climate changes information recorded in the study area.

Based on the magnetic susceptibility analysis, together with references to previous researches on the activity regulation of modern sand dunes in the Mu Us Desert (Li *et al.*, 1998; 2001), the valleys of the magnetic susceptibility values are regarded as cold valleys, which are influenced by East Asia winter monsoon as a result of the high pressure of Siberia-Mongolian anticyclone, and the peaks are regarded as warm peaks, which are influenced by East Asia summer monsoon. Obviously, we should take the 11 layers of dune sands, 0MD, 2PD, 4PD, 6PD, 8PD, 10PD, 12PD, 14PD, 16PD, 18PD and 20PD, as the phases dominated by winter monsoon (corresponding to C1–C11 in Fig. 1). Accordingly, we should take another 11 layers of fluvio-lacustrine facies

and paleosols, 1PS/LS, 3LS, 5LS, 7LS, 9LS, 11PS, 13LS/FL, 15FL, 17FL, 19FL and 21FL, as the phases dominated by summer monsoon (corresponding to W1–W11 in Fig. 1).

If we calculate the average time for climate cycles of the MGS1 segment in Milanggouwan section in the Holocene, each cycle experienced nearly 1 kyr, namely, there appeared warm and cold climate alternation at a average time of 0.6–0.5 kyr B.P. since 12 kyr B.P. Evidently, the magnetic susceptibility cycles have recorded the ka-scale climate fluctuations in the Salawusu River valley during the Holocene.

As for the climate changes in the North Atlantic, there also existed high-resolution climate changes similar to those of the MGS1 segment in the Milanggouwan section in the Holocene. On the basis of the study on the stained hematite, glass debris in the deep sea sediment of North Atlantic, Bond *et al.* (1997) identified that there existed eight times of IRD (ice-rafted debris) events there in the Holocene, and the times of the peak occurrence are 1.4 kyr, 2.8 kyr, 4.3 kyr, 5.9 kyr, 8.2 kyr, 9.5 kyr, 10.3 kyr and 11.1 kyr, around cyclic time of 1 470 yr. By comparison (Fig. 2), it is not difficult to find that the climate changes indicated by the magnetic susceptibility of the MGS1 segment in the Salawusu River valley have a good correlation with that of the North Atlantic, in terms of the time and nature of climate. Figure 2 shows that the IRD peaks in the North Atlantic were almost consistent with all the low magnetic susceptibility values of MGS1, in terms of the time, especially 4PD, 10PD, 12PD, 16PD and 18PD perfectly corresponding to the related peaks. The valleys between the peaks in the IRD can be regarded as a warm valley, which exactly correspond to the warm peaks of the magnetic susceptibility value of MGS1. Interestingly, whether the warm period indicated by the significant warm valley around 7 kyr B.P. in the North Atlantic in the Holocene corresponds to the warm peaks of the magnetic susceptibility of 13LS/FL in MGS1 (6 170 yr B.P. of ¹⁴C calendar year) is not clear. Although the latter is a weak warm peak, this section contains much Gastropoda fossils such as *Gyraulus albus* Muller, *Radix* sp., *Gyraulus convexiusculus* Hutton (Li *et al.*, 1998), especially the current species of *Gyraulus convexiusculus* Hutton are widely living in tropical and subtropical zones of China, which reflects the Megathermal

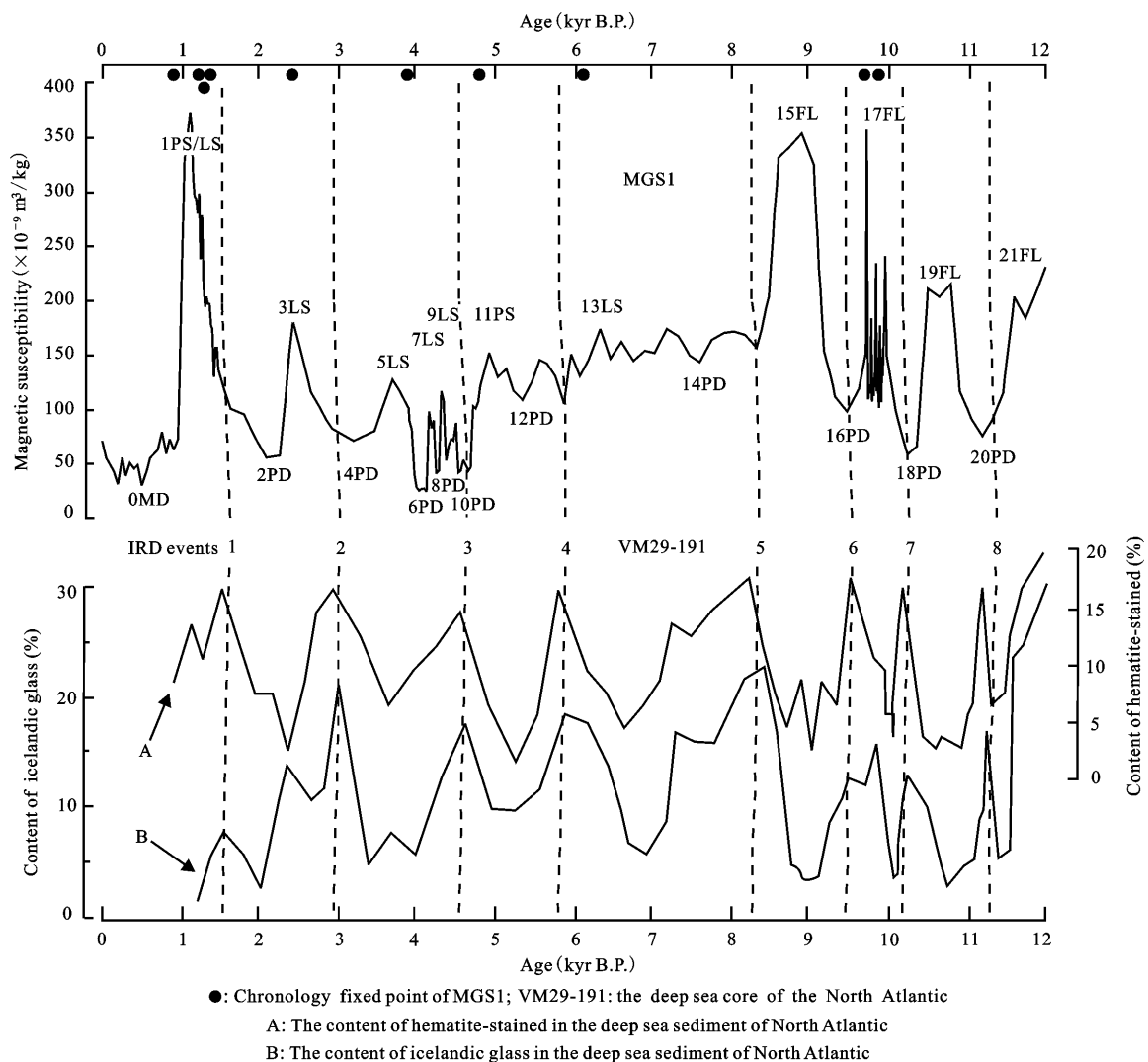


Fig. 2 Comparison between magnetic susceptibility curve of MGS1 and cold-warm events of North Atlantic

ancient climate information. But, whether the weak warm peak is related to an increase of fossil gastropods diluting the ferromagnetic minerals is still in question.

In fact, high-resolution cold events in many locations of China in the Holocene have been confirmed, such as cold events recorded in the Huguangyan (Liu *et al.*, 2000), Zoigê (Zhou *et al.*, 2001), Dundee (Yao and Shi, 1992), and similar incidents were also found in Okinawa, Japan (Jian and Meng, 2002). These events also have a good correlation with the time of cold valley of magnetic susceptibility value in MGS1 (calculated by deposition rate interpolation) (Table 4). The warm events were consistent with warm climate in other parts of China, in terms of the time of occurrence, for example, the paleosol developing around 6.1 kyr B.P. and 1.3–0.7 kyr B.P. in Hunshandake Desert (Jin *et al.*, 2004) corre-

sponded to 13LS/FL and 1PS/LS, respectively, and the latter displayed as an extreme value of the high magnetic susceptibility. Moreover, Daihai Lake level significantly elevated from 1.2 kyr B.P. to 0.9 kyr B.P. (Jin *et al.*, 2002), whose time is also roughly equivalent to the age of the extreme high magnetic susceptibility. It shows that 11 cycles of magnetic susceptibility valley-peak alternating, which appears vertically in the sedimentary cycles of MGS1, reflect 11 cycles of warm-cold climate alternation.

The fact that the cold valleys and the warm peaks of the magnetic susceptibility in the MGS1 couple with cold peaks and warm valleys in the North Atlantic, as well as cold-warm changes in some of places of China, in terms of time, reflects that these millennial-centennial scales climate changes may basically result from global

Table 4 Comparison of cold events in Holocene (yr B.P.)

MGS1 horizon	MGS1 horizon chronology*	North Atlantic (Bond <i>et al.</i> , 1997)	Huguangyan (Liu <i>et al.</i> , 2000)	Zoigê (Zhou <i>et al.</i> , 2001)	Dunde (Yao and Shi, 1992)	Okinawa (Jian and Meng, 2002)
0MD	960–0		680		400	600
1PS/LS	1350–960					
2PD	2240–1350	1400	1640	1500	1500	1700
3LS	2470–2240					
4PD	3530–2470	2800	2680	2800	3000	3300
5LS	4000–3530					
6PD	4180–4000		3830	3700		
7LS	4290–4180					
8PD	4350–4290					
9LS	4380–4350					
10PD	4760–4380	4300		4400	4000	4600
11PS	5040–4760					
12PD	5920–5040	5900	5040, 6290	6400	5400	5900
13LS/FL	6570–5920					
14PD	8270–6570	8200	8680	8900	8700–8900	8100
15FL	9020–8270					
16PD	9700–9020	9500	9830	9580	9700	9400
17FL	9880–9700					
18PD	10160–9880	10300		10200		
19FL	10580–10160					
20D	11080–10580	11100				
21FL	11950–11080					

Note: * is interpolated by the average sedimentary ratios calculated separately through sediment thickness between two ages

high-resolution climate fluctuations in the Holocene. When it turned cold globally, the Salawusu River valley was subjected to the strong winter monsoon, thus the surface ferromagnetic materials were diluted and magnetic susceptibility values were low due to the physical weathering, erosion and accumulation of the drift sands. As it turned warm globally, the summer monsoon prevailed there with strongly biochemical weathering, which resulted in sediments in the rivers and lakes, development of paleosols and relative accumulation of surface ferromagnetic materials with high value of magnetic susceptibility.

5 Conclusions

The distribution of magnetic susceptibility of MGS1 in the Salawusu River Valley obviously corresponds to 11 sedimentary cycles of sand dunes and the overlying fluvio-lacustrine facies or paleosols, with a good peak-valley correspondence. On the basis of the analysis on the significance of magnetic susceptibility to the climate and environment, this paper suggests that the valleys and the peaks reflect the cold-dry winter monsoon climate and

the warm-humid summer monsoon climate, respectively. In millennial-centennial scales, the MGS1 segment has totally recorded 22 periods of climate alternations from the cold-arid to the warm-humid in the study area during the Holocene. In terms of the time and the climate nature, the variations similarly correspond to those of the North Atlantic and some records of cold-warm changes in China as well. It indicates that the climate change at millennial-centennial scales in the Salawusu River Valley and the Mu Us Desert in the Holocene was influenced by global and regional climate, and it was an integral part of global millennial-centennial scales climate fluctuations, which can serve as a standard climate stratigraphy sample for comparison with warm-cold climate events at the same periods in other sandy areas of China.

Acknowledgements

We thank Professor Jin Heling, Professor Li Shen for their help and advice, and great gratitude to Ms. Lu Liangcai and Wang Guangxin for their analysis and determination of the TL ages and mineral detritus dating of the samples.

References

- Bond G, Showers W, Cheseby M *et al.*, 1997. A pervasive millennial-scale cycle in North Atlantic Holocene and glacial climates. *Science*, 278(534): 1257–1266. DOI: 10.1126/science.278.534-0.1257
- Chen Fahu, Zhu Yan, Li Jijun *et al.*, 2001. Abrupt Holocene changes of the Asian monsoon at millennial- and centennial-scales: Evidence from lake sediment document in Minqin Basin, NW China. *Chinese Science Bulletin*, 46(17): 1414–1419. (in Chinese)
- Dong Guangrong, Gao Shangyu, Li Baosheng, 1982. New discovery of the Fossil Ordos Man. *Chinese Science Bulletin*, 26(19): 1192–1194. (in Chinese)
- Dong Guangrong, Li Baosheng, Gao Shangyu, 1983. The case study of the vicissitude of Mu Us Sandy Land since the Late Pleistocene according to the Salawusu River strata. *Journal of Desert Research*, 3(2): 9–14. (in Chinese)
- Editorial Board of National Atlas of China, 1965. *The National Physical Atlas of China*. Beijing: China Cartographic Publishing House, 8–9. (in Chinese)
- Guo Zhengtang, Petit N, Liu Dongsheng, 1999. Holocene abrupt environmental changes in the arid regions in Africa and Asia. *Journal of Paleogeography*, 1(1): 68–74. (in Chinese)
- Jia Lanpo, 1950. *The Ordos Fossil Man*. Shanghai: Longmen United Publishing House, 1–89. (in Chinese)
- Jian Zhimin, Meng Yi, 2002. Holocene paleoenvironmental changes in the Yangtze River mouth and their responses to the variations in the Kuroshio Current. *Marine Geology & Quaternary Geology*, 22(3): 77–82. (in Chinese)
- Jin Heling, Li Mingqi, Su Zhizhu *et al.*, 2007. Sedimentary age of strata in the Salawusu River Basin and climatic changing. *Acta Geologica Sinica*, 81(3): 307–315. (in Chinese)
- Jin Heling, Su Zhizhu, Sun Liangying *et al.*, 2004. Climate change of Holocene in Hunshandake desert. *Chinese Science Bulletin*, 49(15): 1532–1536. (in Chinese)
- Jin Zhangdong, Shen Ji, Wang Sumin *et al.*, 2002. The medieval warm period in the Daihai area. *Journal of Lake Sciences*, 14(3): 209–216. (in Chinese)
- Kukla G, 1987. Loess stratigraphy in Central China. *Quaternary Science Reviews*, 6(3–4): 191–207, 209–219. DOI: 10.1016/0277-3791(87)90004-7
- Li Baosheng, Zhang David Dian, Jin Heling *et al.*, 2000. Paleo-monsoon activities of Mu Us Desert, China since 150 ka B.P.—A study of the stratigraphic sequences of the Milangouwan Section, Salawusu River area. *Palaeogeography, Palaeoclimatology, Palaeoecology*, 162: 1–16. DOI: 10.1016/S0031-0182(00)00101-2
- Li Baosheng, Dong Guangrong, Gao Shangyu *et al.*, 1987. Relationship between the Malan Loess and the Salawusu Formation in the Salawusu River area, Ordos and their geological ages. *Acta Geologica Sinica*, (3): 218–230. (in Chinese)
- Li Baosheng, Dong Guangrong, Wu Zheng *et al.*, 1993. The establishment of the Upper Pleistocene Chengchuan Formation in northern China. *Geological Review*, 39(2): 91–100. (in Chinese)
- Li Baosheng, Jin Heling, Lu Haiyan *et al.*, 1998. Processes of the deposition and vicissitude of Mu Us Desert, China since 150,000 a B.P. *Science in China (Series D)*, 28(1): 85–90. (in Chinese)
- Li Baosheng, Jin Heling, Zhu Yizhi *et al.*, 2004. The Quaternary lithostrata in Salawusu River Valley and their geochronology. *Acta Sedimentologica Sinica*, 22(4): 676–682. (in Chinese)
- Li Baosheng, Wu Zheng, David Dian Zhang *et al.*, 2001. Environment and its changes in the monsoon sandy region of China during the Late Pleistocene and Holocene. *Acta Geologica Sinica*, 75(1): 127–137. (in Chinese)
- Liu Jiaqi, Lu Houyuan, Negendank J *et al.*, 2000. Periodicity of Holocene climatic variations in the Huguangyan Maer Lake. *Chinese Science Bulletin*, 45(11): 1190–1195. (in Chinese)
- Liu Xiuming, Liu Tungsheng, Heller F *et al.*, 1990. Frequency-dependent susceptibility of loess and quaternary paleoclimate. *Quaternary Sciences*, (1): 42–50. (in Chinese)
- Liu Yufei, Li Baosheng, Yang Yi *et al.*, 2006. Moving and accumulating law of Rb, Sr with environment evolving in semiarid basin of China during the last interglacial—Reflected by study result on Milangouwan stratigraphic section in the Salawusu River valley. *Journal of Desert Research*, 26(3): 341–344. (in Chinese)
- Niu Dongfeng, Li Baosheng, Du Shuhuan *et al.*, 2008. Cold events of Holocene indicated by primary elements distribution of the high-resolution sand dunes in the Salawusu River Valley. *Journal of Geographical Sciences*, 18: 26–36. DOI: 10.1007/s11442-008-0026-4.
- O'Brien S R, Mayewski P A, Meeker L D *et al.*, 1995. Complexity of Holocene climate as reconstructed from a Greenland ice core. *Science*, 270(5244): 1962–1964. DOI: 10.1126/science.270.5244.1962
- Ouyang Chuntao, Li Baosheng, Ou Xianjiao *et al.*, 2007. Chemical weathering of the Milangouwan paleosols in the Salawusu River Valley and their paleoclimatic implication during the Last Interglacial Period. *Acta Geographica Sinica*, 62(5): 518–528. (in Chinese)
- Pei Wenzhong, Li Youheng, 1964. Some tentative opinions on the problem of "Sjara-Osso-Gol Series". *Vertebrata Palasiatica*, 8(2): 99–118. (in Chinese)
- Qi Guoqin, 1975. Quaternary mammalian fossils from Salawusu River District, Nei Mongol. *Vertebrata Palasiatica*, 13(4): 239–249. (in Chinese)
- Su Zhizhu, Dong Guangrong, 1994. Recent progress on Quaternary research of Salawusu River area in Inner Mongolia. *Arid Land Geography*, 17(4): 1–8. (in Chinese)
- Stuiver M, Reimer P J, Bard E *et al.*, 1998. INTCAL98 Radiocarbon age calibration 24,000-0 cal BP. *Radiocarbon*, 40: 1041–

- 1083.
- Su Zhizhu, Dong Guangrong, Li Xiaoqiang *et al.*, 1999. The lake-swamp sediment records on the environmental characteristics of Mu Us Desert since the Late Glacial Epoch. *Journal of Desert Research*, 19(2): 104–109. (in Chinese)
- Taylor K C, Lamorey G A, Doyle R B *et al.*, 1993. The 'flickering switch' of Late Pleistocene climate change. *Nature*, 361: 432–436.
- Teilhard de Chardin P, Licent E, 1924. On the discovery of a Paleolithic industry in Northern China. *Bulletin of the Geological Society of China*, 3(1): 45–50.
- Wang L, Sarnthein M, Erlenkeuser H *et al.*, 1999. East Asian monsoon climate during the Late Pleistocene: High-resolution sediment records from the South China Sea. *Marine Geology*, 156: 245–284. DOI: 10.1016/S0025-3227(98)00182-0
- Woo Jukang, 1958. Fossil human parietal bone and femur from Ordos. *Vertebrata Palasiatica*, 2(1): 208–210. (in Chinese)
- Xian Feng, Zhou Weijian, Yu Xuefeng *et al.*, 2006. Evidence for abrupt changes of the Asian monsoon during the Holocene: From the peat records of Tibetan Plateau. *Marine Geology & Quaternary Geology*, 26(1): 41–45. (in Chinese)
- Yao Tandong, Shi Yafeng, 1992. Climatic changes of Holocene reflected in the ice core from Dunde, Qilian Mountains. In: Shi Yafeng *et al.* (eds.). *The Climates and Environments of Holocene Megathermal in China*. Beijing: China Ocean Press, 206–211. (in Chinese)
- Yuan Baoyin, 1978. Sedimentary environment and stratigraphical subdivision of Sjara Osso-Gol formation. *Scientia Geologica Sinica*, (3): 220–234. (in Chinese)
- Yuan Sixun, Chen Tiemei, Gao Shijun, 1983. Uranium series dating of "Ordos Man" and "Sjara-Osso-Gol" culture. *Acta Anthropologica Sinica*, 2(1): 90–94. (in Chinese)
- Zhou Kunshu, Li Xingguo, Shao Yajun, 1982. The permafrost period subdivision in the Salawusu River reaches, Inner Mongolia, and its significance. In: *Contribution to the Academic Symposium on the Pre-Historic Earthquake and Geology of China*. Xi'an: Shaanxi Science and Technology Press, 149–153. (in Chinese)
- Zhou Weijian, Lu Xuefeng, Wu Zhengkun *et al.*, 2001. Peat record reflecting Holocene climatic change in the Zoigê Plateau and AMS radiocarbon dating. *Chinese Science Bulletin*, 46(12): 1040–1044. (in Chinese)